arXiv:cond-mat/0201487v1 [cond-mat.mes-hall] 26 Jan 2002

Magnetic Polarization Currents in Double Quantum Dot Devices

Sam Young Cho[1], Ross H. McKenzie[1], Kicheon Kang[2], and Chul Koo Kim[3]
[1]*Department of Physics, University of Queensland, Brisbane 4072, Australia*
[2]*Basic Research Laboratory, Electronics and Telecommunications Research Institute, Taejon 305-350, Korea*
[3]*Institute of Physics and Applied Physics, Yonsei University, Seoul 120-749, Korea*

(December 23, 2013)

We investigate coherent electron transport through a parallel circuit of two quantum dots, each of which has a single tunable energy level. Electrons tunneling via each dot from the left lead interfere with each other at the right lead. It is shown that due to the quantum interference of tunneling electrons the double quantum dot device is magnetically polarized by coherent circulation of electrons on the closed path through the dots and the leads. Varying the energy level of each dot one can make the magnetic states of the device to be either *up*-, *non*-, or *down*- polarization. It is shown that for experimentally accessible temperatures and applied biases the magnetic polarization currents should be sufficiently large to observe with current nanotechnology.

PACS numbers: 73.23.Hk, 73.63.Kv, 73.40.Gk, 85.35.Ds

The most interesting phenomena seen in mesoscopic electronic devices are due to the quantum coherence of electrons being maintained over a significant part of the transport process. Examples of such interference effects [1] that have been observed include weak localization, universal conductance fluctuations, and Aharonov-Bohm (AB) oscillations. In 1995, Yacoby and coworkers [2] demonstrated the coherence of electron waves passing by resonant tunneling through a quantum dot (QD) in a double-slit type interference in a ring geometry. Recent interference experiments [3–5] with two different transport paths in a ring geometry have enabled the realization of a phase sensitive probe of the effects of electron-electron interaction on the conductance oscillation such as Kondo correlations [5–9], as well as the anomalous phase of the transmission coefficients through a QD [10–15]. Two QDs have also been fabricated experimentally on two different electron pathways [16]. These double quantum dot (DQD) devices provide a good opportunity to test theories of resonant tunneling [17,18], cotunneling [19–21], and many-body correlation effects [22,23]. Compared to ballistic electron interference devices [24,25], a DQD device makes it possible to manipulate the coherent tunneling of electrons through each dot separately by varying the gate voltages of the dots. König and Gefen [21] have discussed quantum coherence in DQD devices with the *same* energy level in each dot.

In this Letter, we study coherent electron transport through two parallel QDs, each of which has a single *tunable* energy level (see Fig. 1). Remarkably, we find a coherent magnetic polarization current (MPC) circulating on the closed path connecting the dots and the leads as a function of each dot level position. This MPC is induced by coherent tunneling for electron transport through each QD. We discuss the magnetic polarizability of the DQD device due to the MPC for finite temperature and finite applied bias.

We start with the model Hamiltonian

$$H=\sum_{\substack{k\in L,R\\ \sigma}}\varepsilon_k c^\dagger_{k\sigma}c_{k\sigma}+\sum_{\substack{i\in 1,2\\ \sigma}}\varepsilon_i d^\dagger_{i\sigma}d_{i\sigma}+\sum_{\substack{i\in 1,2\\ k\sigma\in L,R}}(V_k c^\dagger_{k\sigma}d_{i\sigma}+\text{h.c.}), \quad (1)$$

where $c_{k\sigma}$ and $d_{i\sigma}$ are the annihilation operators with spin σ for electrons in the leads and the dots ($i=1,2$), respectively. ε_1 and ε_2 are the level energy in each dot, measured, relative to the Fermi energy of the leads. The symmetric tunnel-coupling between the dots and the leads will be assumed to be independent of energy, $|V_k|=|V|$.

The current flowing into the each quantum dot can be defined as the rate of change in the number of electrons in a lead. At the left lead L, the total current is split into two local currents, I_1 and I_2. The commutator of the number operator $N=\sum_{k\sigma\in L}c^\dagger_{k\sigma}c_{k\sigma}$ with the Hamiltonian (1) gives rise to the current as the sum of the local currents through each dot,

$$I=\sum_{i=1,2}I_i, \quad (2a)$$

$$I_i=-\frac{e}{h}\text{Re}\Big\{\sum_{k\sigma\in L}\int d\varepsilon\, V_k\, G^<_{k\sigma,i\sigma}(\varepsilon)\Big\} \quad (2b)$$

with the nonequilibrium Green's function $G^<_{k\sigma,i\sigma}(t-t')\equiv i\langle d^\dagger_{i\sigma}(t')c_{k\sigma}(t)\rangle$. With the Keldysh technique for nonlinear current through the system, the local currents through each dot are given by [26,27]

$$I_i=\frac{e}{h}\sum_\sigma\int d\varepsilon\,(f_L(\varepsilon)-f_R(\varepsilon))\mathcal{T}_i(\varepsilon), \quad (3)$$

where the local transmission spectral functions are defined by $\mathcal{T}_i(\varepsilon)=\big\{\mathbf{\Gamma}^L\mathbf{G}^\text{r}_\sigma(\varepsilon)\mathbf{\Gamma}^R\mathbf{G}^\text{a}_\sigma(\varepsilon)\big\}_{ii}$ which is the i-th diagonal component of the matrix transmission spectral function. Here, $f_\alpha(\varepsilon)=f(\varepsilon-\mu_\alpha)$ is the Fermi-Dirac distribution function of the leads $\alpha=L,R$ and $\mu_L=-\mu_R=eV/2$ with applied bias eV between two leads. Due to tunneling each dot level acquires a finite line width $\Gamma=2\pi|V|^2\mathcal{N}$, where $\mathcal{N}$ is the density

of states in the leads. The matrix coupling to the leads is described by $\mathbf{\Gamma}^L = \mathbf{\Gamma}^R = \Gamma \begin{pmatrix} 1 & 1 \\ 1 & 1 \end{pmatrix}$. $\mathbf{G}^{\rm r}_\sigma(\varepsilon)$ is the matrix dot Green's function defined in time space as $G^{\rm r}_{ij,\sigma}(t-t') = -i\theta(t-t')\langle\{d_{i\sigma}(t), d^\dagger_{j\sigma}(t')\}\rangle$. By using the equation of motion treatment, one can obtain the matrix Green's function of the dots as

$$\mathbf{G}^{\rm r}_\sigma(\varepsilon) = \begin{pmatrix} \varepsilon - \varepsilon_1 + i\Gamma & i\Gamma \\ i\Gamma & \varepsilon - \varepsilon_2 + i\Gamma \end{pmatrix}^{-1} \tag{4}$$

and $\mathbf{G}^{\rm a}_\sigma(\varepsilon) = [\mathbf{G}^{\rm r}_\sigma(\varepsilon)]^\dagger$. Accordingly, the local transmission spectral functions are written by

$$\mathcal{T}_1(\varepsilon) = \frac{\Gamma^2(\varepsilon-\varepsilon_2)(2\varepsilon-\varepsilon_1-\varepsilon_2)}{(\varepsilon-\varepsilon_1)^2(\varepsilon-\varepsilon_2)^2 + (2\varepsilon-\varepsilon_1-\varepsilon_2)^2\Gamma^2}\,, \tag{5a}$$

$$\mathcal{T}_2(\varepsilon) = \frac{\Gamma^2(\varepsilon-\varepsilon_1)(2\varepsilon-\varepsilon_1-\varepsilon_2)}{(\varepsilon-\varepsilon_1)^2(\varepsilon-\varepsilon_2)^2 + (2\varepsilon-\varepsilon_1-\varepsilon_2)^2\Gamma^2}. \tag{5b}$$

Note that these can be negative. The total current is the sum of current through each dot $I = I_1 + I_2$ which is just the current conservation. This leads to the total transmission spectral function as $\mathcal{T}(\varepsilon) = \mathcal{T}_1(\varepsilon) + \mathcal{T}_2(\varepsilon)$,

$$\mathcal{T}(\varepsilon) = \frac{\Gamma^2(2\varepsilon-\varepsilon_1-\varepsilon_2)^2}{(\varepsilon-\varepsilon_1)^2(\varepsilon-\varepsilon_2)^2 + (2\varepsilon-\varepsilon_1-\varepsilon_2)^2\Gamma^2}\,. \tag{6}$$

We note that this is always positive. The classical analogue of our system is two resistors in parallel. I_1 and I_2 must then both be positive. In contrast, in a quantum system the only constraint is that current conservation requires $I = I_1 + I_2$. It is not required that $I > I_1,\ I_2$. For the case of a metallic ring coupled to leads, this was pointed out previously by Jayannavar and Deo [28]

Let us assume the cases of $I < I_1$ or $I < I_2$ under the current conservation for $\mu_R < \mu_L$. For given energy levels $(\varepsilon_1, \varepsilon_2)$, if $I(\varepsilon_1,\varepsilon_2) < I_1(\varepsilon_1,\varepsilon_2)$, we can assign an excess current $I_{exc}(\varepsilon_1,\varepsilon_2)$. Then we can rewrite the total current as $I(\varepsilon_1,\varepsilon_2) = I_1(\varepsilon_1,\varepsilon_2) - I_{exc}(\varepsilon_1,\varepsilon_2)$. The current conservation gives rise to the local excess current of $I_{exc}(\varepsilon_1,\varepsilon_2) = -I_2(\varepsilon_1,\varepsilon_2)$ which should circulate *clockwise* on the closed path through the dots and the leads. In the opposite case of $I < I_2$, the excess current becomes $I_{exc}(\varepsilon_1,\varepsilon_2) = -I_1(\varepsilon_1,\varepsilon_2)$ circulating *counter-clockwise* on the closed path. The circulating current makes the device magnetically polarized. Therefore, we define the circulating current as a magnetic polarization current (MPC) $I_M \equiv -I_{exc}$. We choose its direction for the case of $I < I_1$ as *positive*. It should be noted that this is purely a quantum coherent mesoscopic phenomena.

Considering the transport current (TC), I, and MPC, I_M, on an equal footing, we define the MPC as

$$I_M = \frac{-e}{h}\sum_\sigma \int d\varepsilon (f_L(\varepsilon) - f_R(\varepsilon))\mathcal{T}_M(\varepsilon) \tag{7}$$

with the effective spectral function, $\mathcal{T}_M(\varepsilon)$. The $\mathcal{T}_M(\varepsilon)$ can be extracted from the following arguments. Let us recall the transmission spectral functions for $\varepsilon_1 < \varepsilon_2$. $\mathcal{T}(\varepsilon)$ has three extremum points, that is, $\mathcal{T}(\varepsilon_1) = \mathcal{T}(\varepsilon_2) = 1$ (resonant transmission) and $\mathcal{T}(\bar\varepsilon) = 0$ (anti-resonant transmission), where $\bar\varepsilon = (\varepsilon_1+\varepsilon_2)/2$. At $\varepsilon = \bar\varepsilon$, the anti-resonance of $\mathcal{T}(\varepsilon)$ gives rise to a pronounced dip structure originating from the destructive interference between the transmissions through one QD and the other. Such an anti-resonant feature in a transport system with two different transmission channels is well understood as the Fano effect [29]. Next, the two local transmission spectrals of $\mathcal{T}_1(\varepsilon)$ and $\mathcal{T}_2(\varepsilon)$ have three characteristic points, that is, $\mathcal{T}_1(\varepsilon_1) = 1\,[\mathcal{T}_2(\varepsilon_2) = 1]$ and $\mathcal{T}_1(\varepsilon_2) = \mathcal{T}_1(\bar\varepsilon) = 0$ $[\mathcal{T}_2(\varepsilon_1) = \mathcal{T}_2(\bar\varepsilon) = 0]$. These points have nothing to do with resonant and anti-resonant tunneling through each dot. The two local transmission spectral functions only give us information about the local currents. Then we have to determine the behavior of the local spectrals in other energy regions. It is convenient to consider the ratio of the local transmission to the total transmission. The ratios are written by $\mathcal{T}_1(\varepsilon)/\mathcal{T}(\varepsilon) = 1/(1+g(\varepsilon))$ and $\mathcal{T}_2(\varepsilon)/\mathcal{T}(\varepsilon) = 1/(1+g(\varepsilon)^{-1})$, where $g(\varepsilon) = (\varepsilon-\varepsilon_1)/(\varepsilon-\varepsilon_2)$. For $\varepsilon < \varepsilon_1$ and $\varepsilon > \varepsilon_2$, since $0 < g(\varepsilon) < 1$, the ratios are between 0 and 1. In these regions, there are no local excess currents. However, for $\varepsilon_1 < \varepsilon < \bar\varepsilon$, $\mathcal{T}_1(\varepsilon)/\mathcal{T}(\varepsilon) > 1$ $[\mathcal{T}_2(\varepsilon)/\mathcal{T}(\varepsilon) < 0]$ and for $\bar\varepsilon < \varepsilon < \varepsilon_2$, $\mathcal{T}_1(\varepsilon)/\mathcal{T}(\varepsilon) < 0$ $[\mathcal{T}_2(\varepsilon)/\mathcal{T}(\varepsilon) > 1]$. These spectral properties give rise to the MPC at a given energy ε. Similarly, one can decide the $\mathcal{T}_M(\varepsilon)$ for $\varepsilon_1 > \varepsilon_2$. Consequently, we obtain the $\mathcal{T}_M(\varepsilon)$ in terms of the local transmission spectrals as

$$\mathcal{T}_M(\varepsilon) = \sum_{i\neq j}\theta(\varepsilon_i-\varepsilon_j)\Big\{\theta(\varepsilon-\bar\varepsilon)\theta(\varepsilon_i-\varepsilon)\mathcal{T}_j(\varepsilon) - \theta(\varepsilon-\varepsilon_j)\theta(\bar\varepsilon-\varepsilon)\mathcal{T}_i(\varepsilon)\Big\}. \tag{8}$$

Equations (7) and (8) are the central result of this work. Note that, for a given energy level position $(\varepsilon_1,\varepsilon_2)$ in each dot, the $\mathcal{T}_M(\varepsilon)$ is non-zero between the two energy levels $\varepsilon_i < \varepsilon < \varepsilon_j$ and is an anti-symmetric function with respect to $\bar\varepsilon$, $\mathcal{T}_M(\varepsilon-\bar\varepsilon) = -\mathcal{T}_M(\bar\varepsilon-\varepsilon)$. These properties of $\mathcal{T}_M(\varepsilon)$ determine the window of applied bias in which the MPC can be measured.

At zero temperature, the limit of zero applied bias is the most simple case. The TC is proportional to the transmission of incoming electrons at the Fermi energy ($\varepsilon_F = 0$); $\lim_{eV\to 0} I = (2e/h)\mathcal{T}(\varepsilon)|_{\varepsilon=\varepsilon_F} eV$ and the MPC becomes $\lim_{eV\to 0} I_M = (-2e/h)\mathcal{T}_M(\varepsilon)|_{\varepsilon=\varepsilon_F} eV$. When the energy level of one dot is lying below the Fermi energy and that of the other is lying above the Fermi energy, the MPC appears to polarize the DQD device. If both energy levels of dots are below or above the Fermi energy the device is not magnetically polarized. This implies that the interference between the electron and hole channels produces the MPC. Figure 2 shows the magnetic polarization as a function of $(\varepsilon_1/\Gamma, \varepsilon_2/\Gamma)$ for $\mu_R < \mu_L$. It is shown that manipulating the energy level position of each dot, one can magnetize the DQD devices

as *up*-, *non*-, or *down*-polarized. Applying a finite bias between the leads, the properties of $\mathcal{T}_M(\varepsilon)$ change the polarization zone boundaries. A finite applied bias develops a *non*-polarization zone satisfying the conditions of $-eV/2 < |\varepsilon_1 - \varepsilon_2| < eV/2$ or $-eV/2 < \varepsilon_1, \varepsilon_2 < eV/2$. While the *up*-, and *down*-polarization zones are extended to the *non*-polarization zone of the limit of zero applied bias because the electron and hole channels near the Fermi energy within the window of the applied bias contribute to the MPC. It should be noted, when the applied bias is reversed to $\mu_R > \mu_L$, the magnetic moment of the device is reversed.

To illustrate the MPC for finite temperature, we choose a set of energy level position $(\varepsilon_1/\Gamma, \varepsilon_2/\Gamma) = (0.3, -0.9)$ which can be adjusted to other values by varying the gate voltages. In fact, the level positions taken in the same polarization zone do not affect the physics of the MPC but only change its amplitude. We display the MPC and the TC as a function of applied bias for different temperatures in Fig. 3. As the applied bias increases from zero bias, both the TC and the MPC increase linearly. The MPC is always smaller than the TC for these given energy level positions. However, for the case of other energy level positions, the MPC can become larger than the TC (e.g., for $(\varepsilon_1/\Gamma, \varepsilon_2/\Gamma) = (0.5, -0.6)$, $I_M \simeq 5\,I$ at low temperatures). This linear behavior of the MPC shows that the MPC emerges only in nonequilibrium. Further increase of applied bias results in the MPC approaching its maximum value. Eventually, the disappearance of the MPC arises when the window of the applied bias becomes larger than the range of ε for which $\mathcal{T}_M(\varepsilon)$ has a non-zero value $(-0.9 < \varepsilon < 0.3)$. The inset of Fig. 3(b) shows that the TC increases non-linearly as the applied bias increases. In addition, compared to the MPC, the TC is suppressed for the bias smaller than $eV = 0.6\,\Gamma$ but enhanced for the bias larger than $eV = 0.6\,\Gamma$ by thermal effects. This originates from the fact that $\mathcal{T}(\varepsilon)$ has a pronounced dip structure at $\bar{\varepsilon} = -0.3\,\Gamma$, due to the Fano effect. However, the anti-symmetric property of $\mathcal{T}_M(\varepsilon)$ gives rise to moderate thermal suppression of the MPC. The thermal suppression is manifestly shown in the temperature dependence of the MPC and the TC in Fig. 4. The relatively large applied bias leads to the large amplitude of the MPC. This is consistent with the linear behavior of the MPC in the I_M-V curve. The insets of Fig. 4(a) and (b) show, compared to the TC, the more rapid suppression of the MPC since $\mathcal{T}_M(\varepsilon)$ is zero for low and high energies. At $k_BT \simeq 0.05\,\Gamma$, the MPCs at various applied biases start to be suppressed by thermal effects. For temperatures higher than $k_BT \simeq 0.2\,\Gamma$, thermal effects wash out this novel quantum coherent phenomena.

From the experimental parameters measured in Ref. [16]; $\Gamma \simeq 50\,\mu$eV and $\mathcal{A} = 2.52 \times 10^{-13}\mathrm{m}^2$, where $\mathcal{A}$ is a corresponding area to AB oscillation, we can estimate the amplitude of a MPC and an induced magnetic moment, $|\vec{\mu}_D| = \mathcal{A} \cdot I_M$. At the point A in the inset of Fig. 3(a), for $k_BT = 0.1\,\Gamma\,(T \simeq 50\,\mathrm{mK})$, one can estimate $I_M \simeq 0.36\,\mathrm{nA}$, when $eV \simeq 25\mu$eV is applied. The induced magnetic moment of the device becomes $|\vec{\mu}_D| \simeq 9\,\mu_B$, where μ_B is the Bohr magneton. Comparing this estimate of the MPC to recent measurements of persistent currents [25] suggests that the effects we are discussing can be observed with existing nanotechnology.

In summary, we studied coherent electron transport through two parallel quantum dots, each of which has a single tunable energy level. By changing these energy levels in the DQD device one can vary the *sign* and *magnitude* of the magnetic polarization current induced by quantum interference effects. This current is sufficiently large that it should be experimentally observable.

This work was supported by the University of Queensland, the Australian Research Council, and the Korean Science and Engineering Foundation through the Center for Strongly Correlated Materials Research (SNU).

[1] See, for a review, Y. Imry, *Introduction to Mesoscopic Physics* (Oxford University Press, Oxford, New York 1997); S. Datta, *Electronic Transport in Mesoscopic Systems* (Cambridge University Press, New York 1995).
[2] A. Yacoby *et al.,* Phys. Rev. Lett. **74**, 4047 (1995).
[3] R. Schuster *et al.*, Nature **385**, 417 (1997).
[4] W.G. van der Wiel *et al.*, Science **289**, 2105 (2000).
[5] Y. Ji *et al.*, Science **290**, 779 (2000).
[6] U. Gerland *et al.*, Phys. Rev. Lett. **84**, 3710 (2000).
[7] W. Hofstetter, J. König, and H. Schoeller, Phys. Rev. Lett. **87**, 156803 (2001).
[8] K. Kang, and S.-C. Shin, Phys. Rev. Lett. **85**, 5619 (2000).
[9] S. Y. Cho *et al.*, Phys. Rev. B **64**, 033314 (2001).
[10] A. L. Yeyati, and M. Büttiker, Phys. Rev. B **52**, R14360 (1995).
[11] G. Hackenbroich, and H.A. Weidenmüller, Phys. Rev. Lett. **76**, 110 (1996).
[12] C. Bruder, R. Fazio, and H. Schoeller, Phys. Rev. Lett. **76**, 114 (1996).
[13] C.-M. Ryu and S. Y. Cho, Phys. Rev. B **58**, 3572 (1998).
[14] H.-W. Lee, Phys. Rev. Lett. **82**, 2358 (1999).
[15] R. Baltin and Y. Gefen, Phys. Rev. Lett. **83**, 5094 (1999).
[16] A.W.Holleitner *et al.*, Phys. Rev. Lett. **87**, 256802(2001).
[17] T. V. Shahbazyan, and M.E. Raikh, Phys. Rev. B **49**, 17123 (1994).
[18] B. Kubala and J. König, cond-mat/0110524.
[19] H. Akera, Phys. Rev. B **47**, 6835 (1993).
[20] D. Loss, and E.V. Sukhorukov, Phys. Rev. Lett. **84**, 1035 (2000).
[21] J. König, and Y. Gefen, Phys. Rev. Lett. **86**, 3855 (2001).
[22] D. Boese, W. Hofstetter, and H. Schoeller, Phys. Rev. B **64**, 125309 (2001).
[23] W. Hofstetter and H. Schoeller, cond-mat/0108359.

[24] D. Mailly, C. Chapelier and A. Benoit, Phys. Rev. Lett. **70** 2020 (1993).
[25] W. Rabaud *et al.*, Phys. Rev. Lett. **86**, 3124 (2001).
[26] Y. Meir, and N. S. Wingreen, Phys. Rev. Lett. **68**, 2512 (1992).
[27] S. Y. Cho, K. Kang and C.-M. Ryu, Phys. Rev. B **60**, 16874 (1999).
[28] A. M. Jayannavar, and P. Singha Deo, Phys. Rev. B **51**, 10175 (1995).
[29] U. Fano, Phys. Rev. **124**, 1866 (1961).

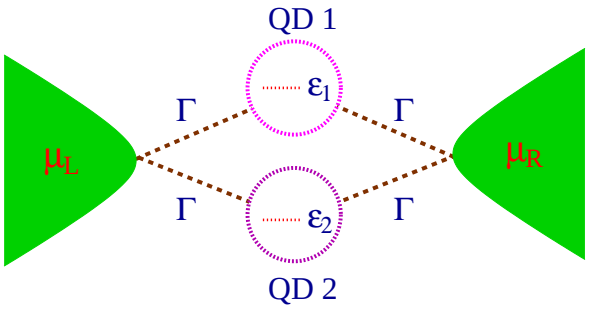


FIG. 1. A double quantum dot (DQD) device. Both dots are tunnel-coupled to the left and right leads. The leads are characterized by the chemical potentials, μ_L and μ_R. The tunneling amplitudes between the dots and the leads are denoted by Γ. The energy level position in each dot is measured as ε_1 and ε_2 from the Fermi energy in the leads.

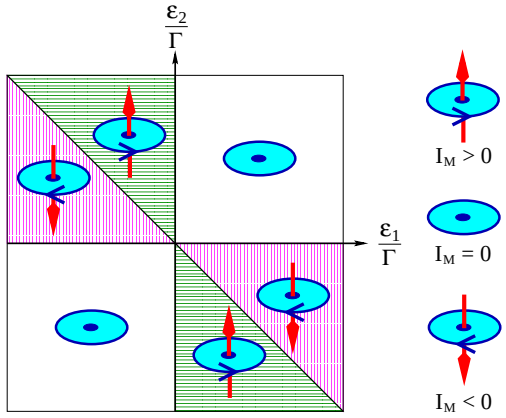


FIG. 2. Magnetic polarization of the double quantum dot device as a function of the energy level positions of each dot $(\varepsilon_1/\Gamma, \varepsilon_2/\Gamma)$, in the limit of zero applied bias at zero temperature for $\mu_R < \mu_L$. The vertical arrows stand for the magnetic moment of the DQD device whose length and direction depends on the amplitude and direction of the magnetic polarization current, respectively.

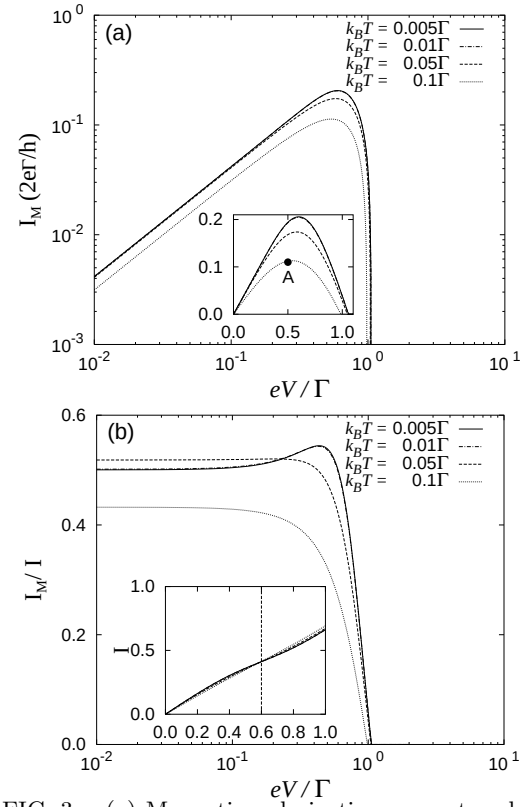


FIG. 3. (a) Magnetic polarization current and (b) its ratio to the transport current as a function of applied bias at $(\varepsilon_1/\Gamma, \varepsilon_2/\Gamma) = (0.3, -0.9)$ for various temperatures k_BT. In the insets, the currents are shown in a linear scale.

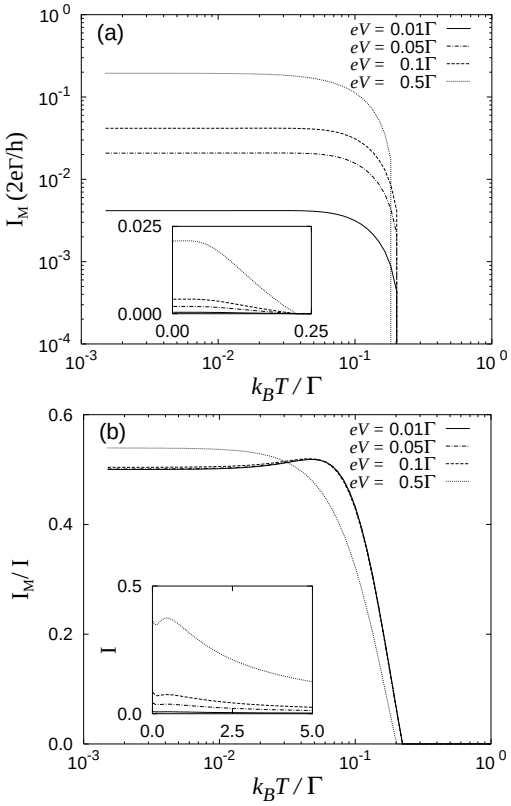


FIG. 4. Temperature dependence of (a) the magnetic polarization current and (b) its ratio to the transport current at $(\varepsilon_1/\Gamma, \varepsilon_2/\Gamma) = (0.3, -0.9)$ for different values of the applied bias eV. In the insets, the currents are shown in a linear scale.